

## Prediction of Waviness Values in Skew Rolling Using Machine Learning Methods

Konrad Lis<sup>1\*</sup>, Zbigniew Pater<sup>1</sup>, Janusz Tomczak<sup>1</sup>, Tomasz Bulzak<sup>1</sup>, Tomasz Kusiak<sup>1</sup>

<sup>1</sup> Department of Metal Forming, Mechanical Engineering Faculty, Lublin University of Technology, 36 Nadbystrzycka Street, 20-618 Lublin, Poland

\* Corresponding author's e-mail: k.lis@pollub.pl

### ABSTRACT

This paper relates to the selection of a machine learning model for predicting the surface waviness of rolled products. An experimental study was carried out using the skew rolling method with three tapered rolls. The products were shaped with variable process parameters. The obtained results were used as a training data set for selected regression models. The random forest model was determined to be the most effective due to the highest value of the coefficient of determination  $R^2$ . The influence of individual process parameters on the waviness value was calculated using the SHAP library.

**Keywords:** skew rolling, waviness, CNC rolling mill, stepped axles and shafts, machine learning.

### INTRODUCTION

Metal forming processes, including cross wedge rolling and skew rolling, are used for manufacturing axisymmetric parts. Examples of products include stepped preforms used in the forging process [1], transmission shaft forgings [2], as well as short stepped shafts [3]. These parts can be made of steels and alloys of non-ferrous metals [4, 5]. A new skew rolling process conducted with three tapered rolls has been developed at the Lublin University of Technology. This process is used for producing stepped axles and shafts. All working tools are described by a forming angle  $\alpha$  and are spaced every  $120^\circ$  on the circumference of the workpiece [Fig. 1]. The rolls are mounted askew to the workpiece axis, at an angle  $\theta$ , and they are rotated with the same velocity in the same direction. The tools move radially relative to the center line of the workpiece. They converge and diverge, thereby reducing the cross section of the workpiece. The spacing of the rolls is synchronized with the axially moving chuck that holds the workpiece by one end. In effect, it is possible to produce parts of variable cross section,

the geometry of which is obtained as a result of sequential motion of the tapered rolls and chuck.

Studies conducted at the Lublin University of Technology have investigated the skew rolling of parts of different shapes. These included preforms of scrapers (for scraper belt conveyors used e.g. in the mining industry), connecting rods and hooks [6]. They were produced in a scale of 1:2 due to design constraints of the laboratory rolling mill. The parts had high dimensional accuracy and were free from internal cracks. In addition, railcar axles were rolled in a scale of 1:5 [7]. These parts were also internal crack-free. In spite of high dimensional accuracy, the rolled parts had small helical grooves on their surface. This, however, is not a serious defect, as the grooves can be removed by machining. Experiments have also been conducted on rolling hollow steel parts with variable cross section [8–10]. The use of hollow tubes made it possible to avoid additional processing operations such as drilling, as well as to prevent unnecessary material loss which occurs when hollow parts are formed from solid billets.

Skew rolling with three tapered rolls makes it possible to produce elongated axisymmetric

parts for the machine-building, aircraft, automotive, and railway industry. The use of cross wedge rolling to the manufacture of such parts is limited by the necessity of constructing working tools with large geometric dimensions. The use of forging is ineffective due to a long forming time. In contrast, the use of the developed skew rolling method to that end ensures reduced manufacture time of these parts, lower energy consumption of the process, as well as reduced costs of constructing new sets of working tools. The process is characterized by the fact that products of different shapes can be rolled with one set of tools. It is only necessary to determine the sequence of movement of tapered rolls and jaw chuck. Due to the universality of the forming tools and the change in their feed rate, the proposed skew rolling technique is cost-effective even with respect to piece production.

The stability of the rolling process depends on parameters such as a forming angle  $\alpha$ , tool angle  $\theta$  relative to the rolling axis, chuck velocity  $V_u$ , and reduction ratio  $\delta$ . Obtained surface quality of rolled parts depends on the initial conditions of the rolling process. Surface texture is described by waviness, roughness and defects such as scratches, cracks or corrosion pits. Its quality may also have impact on further processing of preforms [11]. This means that the initial parameters of rolling must be appropriately selected in order to produce parts of satisfactory quality. This aspect is all the more important when this rolling

process is employed in forging plants, where it is used for fabricating semi-finished parts for further processing or new products. The determination of appropriate values of initial parameters makes it possible to reduce the time of fabrication of acceptable finished parts.

The objective of this study was to assess the effectiveness of selected machine learning models in predicting values of waviness  $W_t$ . This parameter describes surface texture, including peaks and valleys as well as their spacing. The effectiveness of the models was expressed with the coefficient of determination  $R^2$ .

## RESEARCH METHOD

### Scope of experiments

Experiments involved determining the effect of rolling variables on the quality of rolled parts expressed as waviness,  $W_t$ . A schematic design of the rolling process is shown in Figure 1. The billet was a C60 steel rod with a diameter  $d_0 = 52$  mm and a length of 330 mm. The rod was pre-heated to 1200 °C in an electric chamber furnace.

The experiments were conducted with the use of three sets of tapered rolls (Table 1). Each set of the tools had a different forming angle  $\alpha$ , i.e. 15°, 20°, 25°. All rolls had the same sizing part in the form of a cylindrical section with a constant length  $a$ . The rolls were set askew at a variable angle  $\theta$

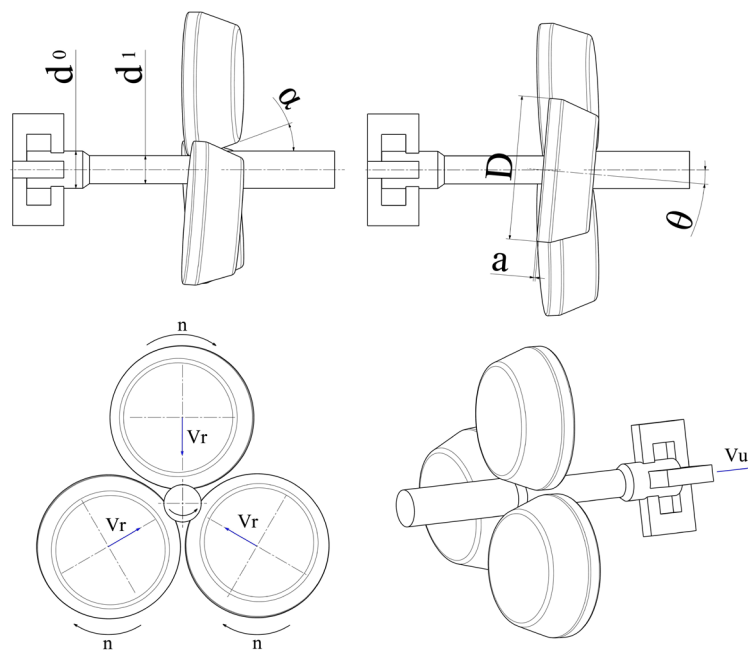


Fig. 1. Schematic representation of a skew rolling process conducted with three tapered rolls

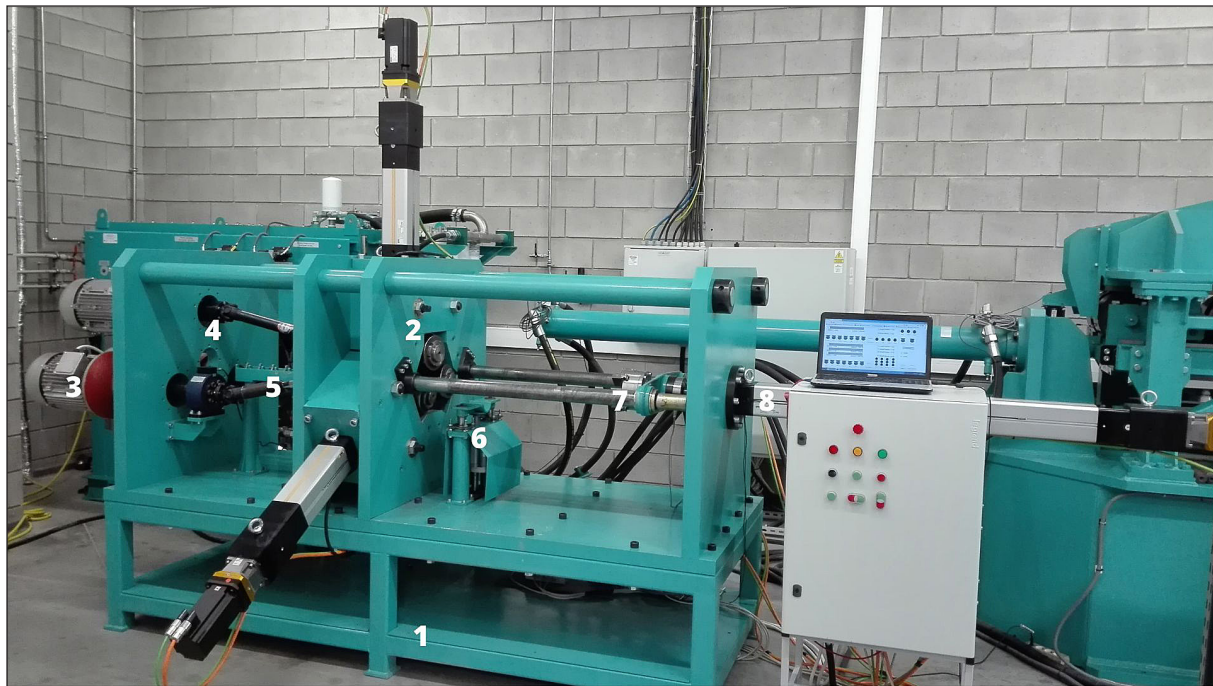


Fig. 2. Laboratory skew rolling mill equipped with three tapered rolls (description in the text)

of 2.5°, 5°, 7.5° relative to the center line of the workpiece. For individual angles of the tapered rolls, the jaw chuck was assigned three different linear velocities  $V_u$ , i.e. 10 mm/s, 20 mm/s and 40 mm/s. Also, three different values of the reduction ratio  $\delta$  were used, i.e. 1.13, 1.3, 1.53. The reduction ratio describes strain and is expressed as:

$$\delta = \frac{d_0}{d_1} \quad (1)$$

where:  $d_0$  – initial billet diameter;  
 $d_1$  – reduced diameter.

The experiments were conducted on a laboratory skew rolling mill (Fig. 2). The test stand has a segment design. The main components of the rolling mill include a frame (1), mill stand (2), drive system (3), powertrain (4), assembly for holding the workpiece (5) and rolled part (6), chuck unit (7), and axial actuator unit (8). The rolling mill was additionally provided with an electric drive. It was also equipped with a measuring system based on the LabVIEW software for force parameters acquisition, including axial and radial loads as well as torque.

The computer numerical control system of this machine makes it possible to form parts with different shapes as a result of sequential motion of the working tools and jaw chuck. The tapered rolls and jaw chuck are moved by electric actuators, and their motion is controlled by a CNC

application that allows visualization of changes in the rolling process parameters [12]. Depending on the shape of the preforms or forgings, it is necessary to create a *dxf* file with the outline

Table 1. Skew rolling parameters used in experiments

$\alpha$ [°]	$\Theta$ [°]	$V_u$ [mm/s]	$\delta$ [-]
15 or 20 or 25	2.5	10	1.13
			1.3
			1.53
		20	1.13
			1.3
			1.53
	40	1.13	
		1.3	
		1.53	
	5	10	1.13
			1.3
			1.53
20		1.13	
		1.3	
		1.53	
40	1.13		
	1.3		
	1.53		
7.5	10	1.13	
		1.3	
		1.53	
	20	1.13	
		1.3	
		1.53	
40	1.13		
	1.3		
	1.53		

of this product. This file will then be converted by the controller into an executive program in the form of a command line (*G-code*), allowing synchronization of the working tools and jaw chuck. Thus, in each operation, a new product differing in external outline can be rolled, still using the same set of tapered rolls.

**Waviness results**

Waviness measurements were made by contact method with Hommel-Etamic’s 3D T8000 RC120-400 profilometer. The waviness  $W_t$  was

measured over a gauge length  $l_n$  of 48 mm with a velocity  $V_t$  maintained constant at 1 mm/s. The selection of individual measurement parameters was made in accordance with the PN-EN ISO 4287:1999 standard.

Figures 3–5 show selected distributions of the waviness  $W_t$  obtained for different reduction ratios, i.e.  $\delta = 1.13$ ,  $\delta = 1.3$  and  $\delta = 1.53$ , with variable forming angle  $\alpha$  and tool angle  $\theta$ . In order to more accurately visualize the changes that have occurred, dot plots connected by lines were used. Examples of obtained outer surfaces of the rolled parts are shown in Figure 6.

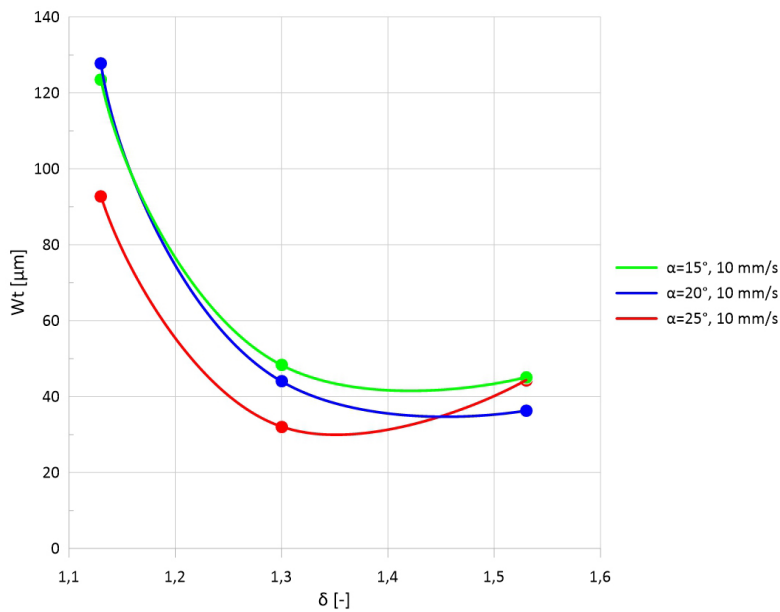


**Fig. 3.** Waviness  $W_t$  of parts rolled with a tool angle of  $\theta = 2.5^\circ$

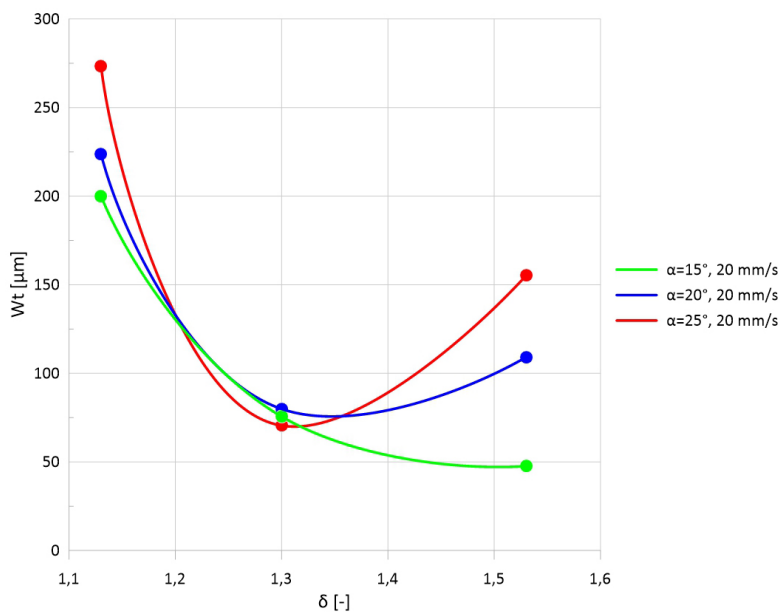


**Fig. 4.** Waviness  $W_t$  of parts rolled with a tool angle of  $\theta = 5^\circ$



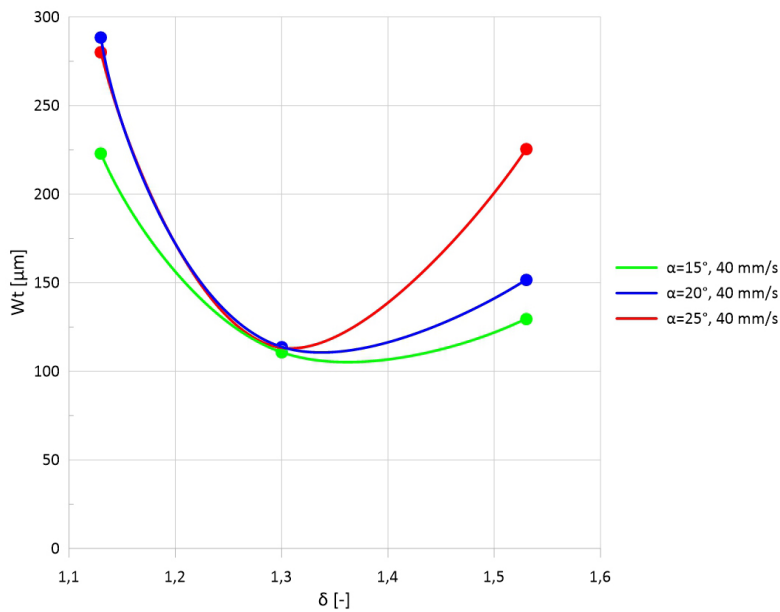


Fig. 5. Waviness  $W_t$  of parts rolled with a tool angle of  $\theta = 7.5^\circ$

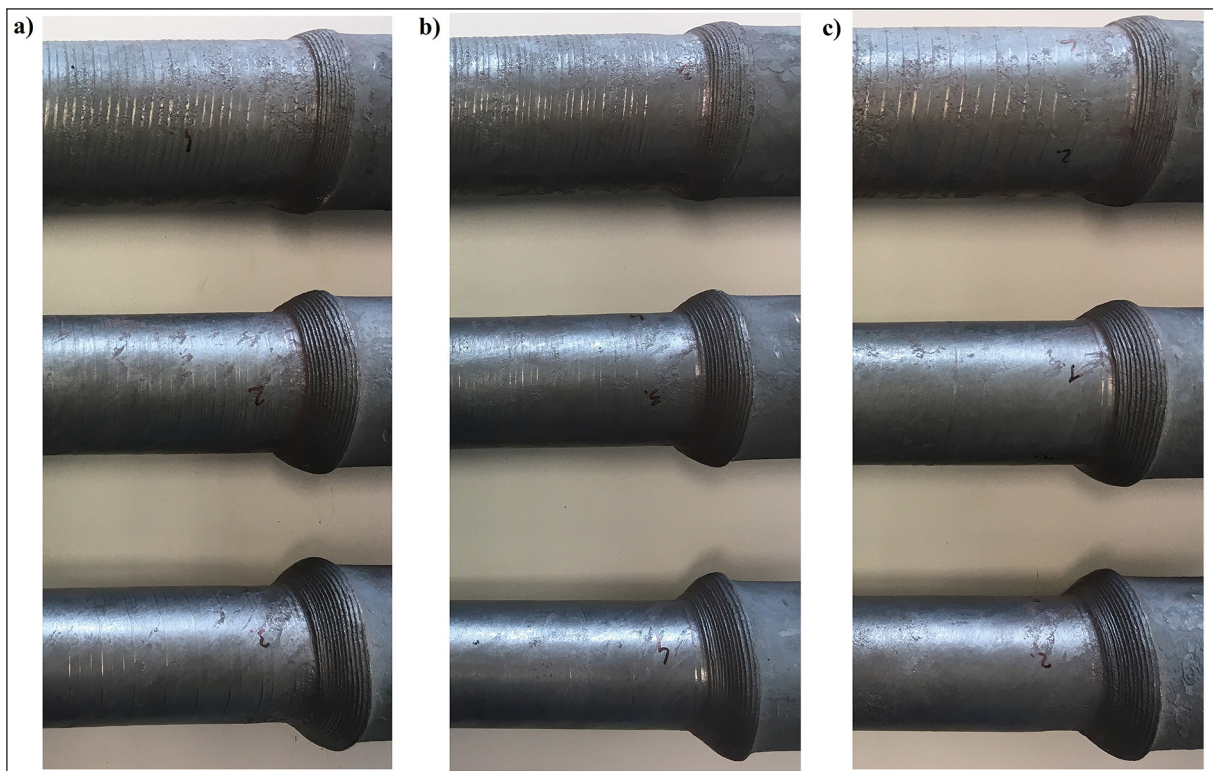


Fig. 6. Outer surface of the parts obtained using tapered rolls with  $\alpha = 15^\circ$  ( $\theta = 5^\circ$ ) and reduction ratios from  $\delta = 1.13$  to  $\delta = 1.53$  (starting from the top): a)  $V_u = 10$  mm/s, b)  $V_u = 20$  mm/s, c)  $V_u = 40$  mm/s

The surface texture examination results showed that an increase in the forming angle  $\alpha$  of the tapered rolls led to a slight increase in the waviness  $W_t$ . The greatest increase was obtained with  $\delta = 1.53$  and the chuck velocities  $V_u = 20$  mm/s and 40 mm/s. On changing the  $\alpha$  angle value from  $15^\circ$  to  $25^\circ$ , the value of  $W_t$  increased by

226% for  $V_u = 20$  mm/s and by 74% for  $V_u = 40$  mm/s. As a result, the increase in  $\alpha$  led to reduced surface quality of the rolled parts. The tool angle  $\theta$  was found to have a significant effect on the waviness  $W_t$ . The waviness value increased with increasing the  $\theta$  angle. To give an example, for the tools with  $\alpha = 15^\circ$  (for  $\delta = 1.3$ ), the  $W_t$  value

increased by 82% when the  $\theta$  angle was increased from  $2.5^\circ$  to  $5^\circ$  and by 42% when the  $\theta$  angle was increased from  $5^\circ$  to  $7.5^\circ$ . The chuck velocity  $V_u$  for different values of the tool angle relative to the rolling axis (for constant  $\alpha$ ) did not have any significant effect on the surface quality of the rolled parts. In contrast, a close relationship was observed between the waviness  $W_t$  and the cross-sectional reduction of the workpiece. The lowest quality surface of the rolled parts was obtained when the rolling process was conducted with the reduction ratio  $\delta = 1.13$ , irrespective of the values of other parameters.

### Description of tested machine learning models

Machine learning methods were used to analyze defects on the surface of rolled products [13]. For this purpose, a classification method was used using models, i.e. Artificial Neural Networks, Support Vector Machines and Decision Trees. The models had high accuracy in predicting defects. The highest value was obtained for Decision Trees equal to 95.9%.

Another example of the application of machine learning methods was the prediction of roughness values of products shaped by the single point incremental forming (SPIF) method [14]. Regression methods using Artificial Neural Networks and Support Vector Regression models were used. In this case, the SVR model was highly effective, achieving a high  $R^2$  coefficient of determination equal to 99%. In comparison, ANN's achieved an  $R^2$  coefficient of 95%.

Therefore, five different machine learning regression models were used in the study, including Linear Regression, k-Nearest Neighbors Regression, Random Forest Regression, Support Vector Regression, and XGBoost. The first four models were taken from the scikit-learn library [15], while the last one from XGBoost [16].

Input data for the models were the skew rolling process parameters, i.e. forming angle  $\alpha$ , tool angle  $\theta$ , chuck velocity  $V_u$ , and reduction ratio  $\delta$ , the values of which are listed in Table 1. The target variable was waviness  $W_t$ . The machine learning dataset constituted 70% of the entire set of variables. The remaining part, i.e. 30%, was a testing dataset. Prediction values were calculated using Google Colaboratory. The effectiveness of the employed models was determined by the coefficient of determination  $R^2$ , defined as:

$$R^2 = 1 - \frac{\sum_{i=1}^n (y_i - \hat{y}_i)^2}{\sum_{i=1}^n (y_i - \bar{y})^2} \quad (2)$$

where:  $y_i$  –  $i$ -th observation of the variable  $y$ ;  
 $\hat{y}_i$  – theoretical value of the variable obtained from the model;  
 $\bar{y}$  – arithmetic mean of the experimental values of the variable.

Input data were subjected to standardization using the StandardScaler function from the scikit-learn library. The operation was performed in compliance with the following:

$$z = \frac{x - \mu}{\sigma} \quad (3)$$

where:  $x$  – experimental value of the input variable;  
 $\mu$  – arithmetic mean of the input data for a given parameter;  
 $\sigma$  – standard deviation of the input data for a given parameter.

The GridSearchCV technique (scikit-learn library) was also employed to select hyperparameters for the selected regression models in order to find best fit.

## RESULTS ANALYSIS

The calculations led to obtaining the coefficient of determination  $R^2$ , the values of which are listed in Table 2.

The highest value of  $R^2 = 0.82$  was obtained for the random forests model. The worst fit was obtained for the k-nearest neighbors model, for which the  $R^2$  value was 0.37. Hence, this model is not considered in further analysis of the results.

A plot illustrating the test and prediction values of waviness obtained for the random forest model is shown in Figure 7.

The effect of individual input variables on the obtained waviness  $W_t$  was also investigated, using the SHAP library [17] and the Shapley value

**Table 2.** Values of the coefficient of determination  $R^2$  for different regression models

Model	$R^2$
Random Forest	0.82
Support Vector Regression	0.75
XGBoost	0.68
Linear Regression	0.67
K-nearest Neighbors	0.37

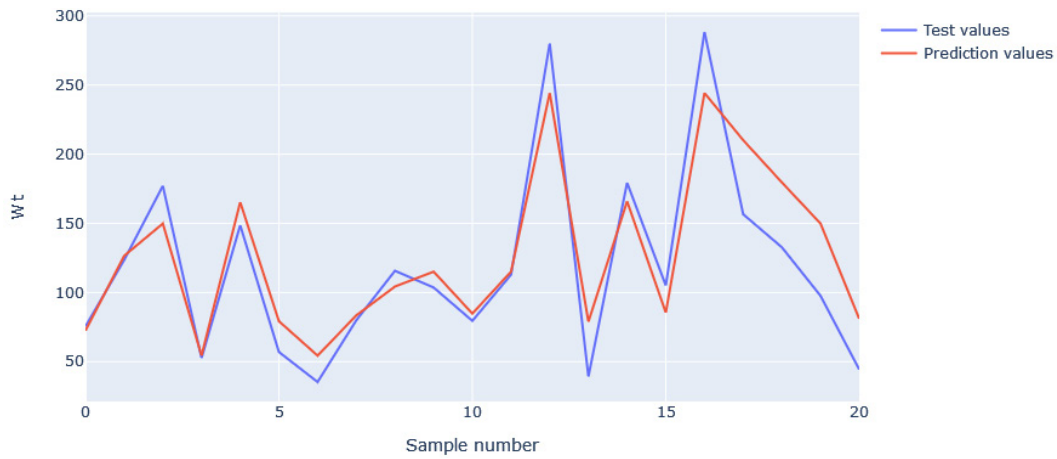


Fig. 7. Test and prediction values of  $W_t$  for a random forest

to that end. Figures 8-11 show the variable significance plots for every tested model. The reduction ratio  $\delta$  and the tool angle  $\theta$  (in this particular order) have the greatest impact on the waviness of the random forests and XGBoost models. As for

other models, i.e. support vector regression and linear regression, the two input variables have a key impact on the waviness of these models yet in a reverse order. It must however be emphasized that their effect on the waviness  $W_t$  changes.

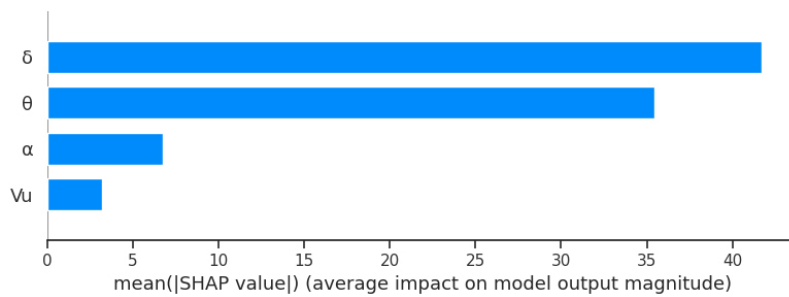


Fig. 8. Variable significance plot for a random forests model

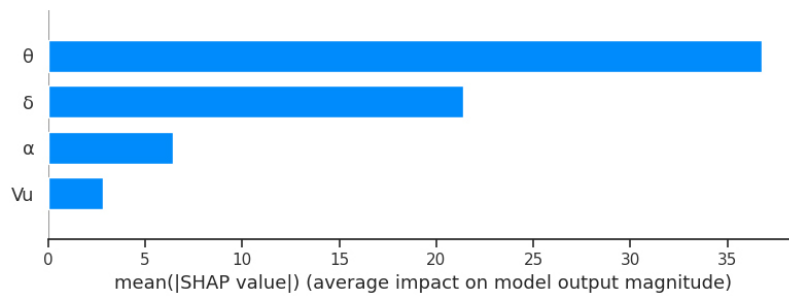


Fig. 9. Variable significance plot for a support vector model

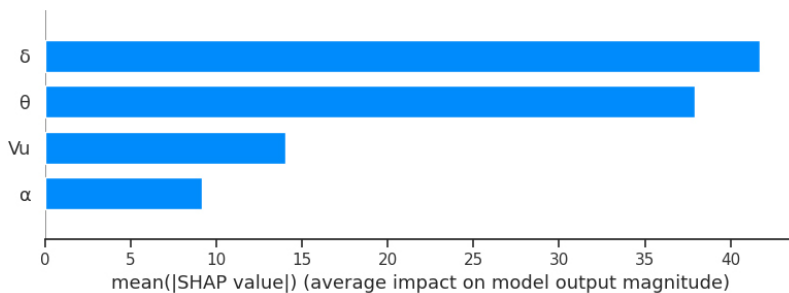


Fig. 10. Variable significance plot for an XGBoost model

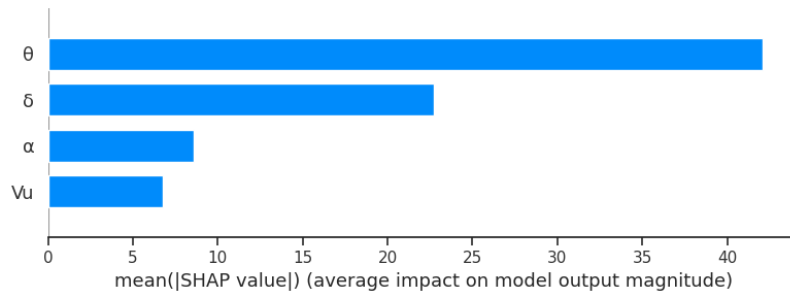


Fig. 11. Variable significance plot for a linear regression model

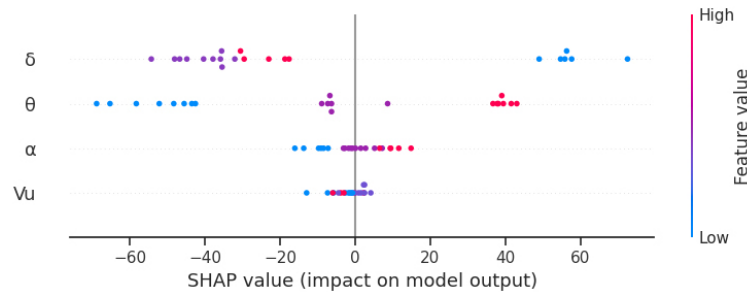


Fig. 12. Effect of variables on the target value, for a random forests model

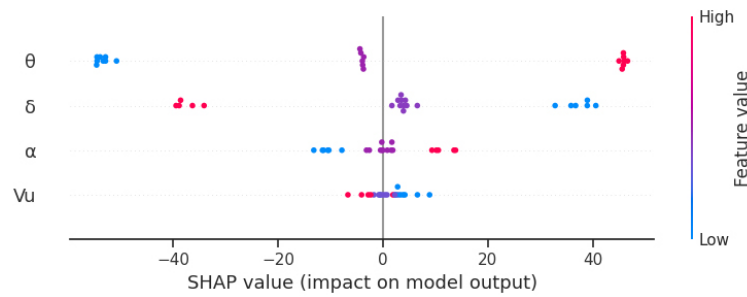


Fig. 13. Effect of variables on the target value, for a support vector model

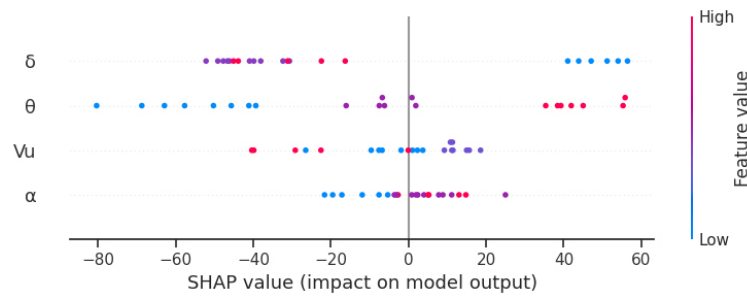


Fig. 14. Effect of variables on the target value, for an XGBoost model

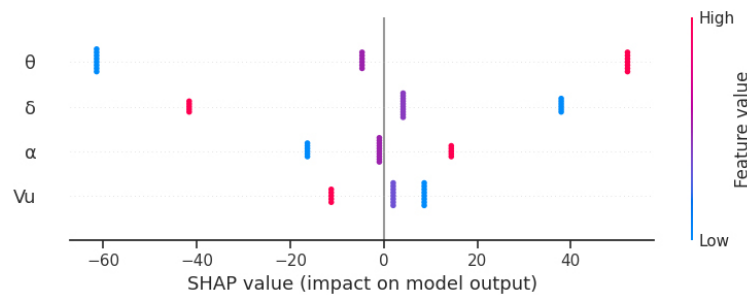


Fig. 15. Effect of variables on the target value, for a linear regression model



The Shapley value of the reduction ratio  $\delta$  is 13% greater than that of the  $\theta$  angle for the random forests model and 10% greater than that of the XG-Boost model. For the support vector model the effect of the tool angle  $\theta$  on the waviness  $W_t$  is 42% higher than that of the reduction ratio  $\delta$ , and for the linear regression model it is 46% higher. The effect of the forming angle  $\alpha$  and the chuck velocity  $V_u$  (it had the lowest Shapley value for the three models) on the obtained target variable is of lesser significance. It can therefore be concluded that these skew rolling parameters should not have any considerable effect on the surface quality of semi-finished and finished parts.

The SHAP library was also used to determine the positive and negative effect of individual input values of the rolling parameters on the target variable  $W_t$  (Figs. 12–15). It can be observed for all regression models that the use of a low reduction ratio ( $\delta = 1.13$ ), high values of the tool angle ( $\theta = 7.5^\circ$ ) and the forming angle  $\alpha = 25^\circ$  leads to a significant increase in the waviness value and thus to reduced surface quality of the rolled parts. Each of these parameters leads to a positive SHAP value. The results demonstrate that the waviness  $W_t$  on the surface of the rolled parts can be decreased by using tools with smaller forming angles, i.e.  $\alpha = 15^\circ$  and  $\alpha = 20^\circ$ . Also, the tool angles  $\theta = 2.5^\circ$  and  $\theta = 5^\circ$  will lead to a decrease in  $W_t$  due to a negative SHAP value.

## CONCLUSIONS

An analysis of the results obtained from the tested machine learning models leads to the following conclusions:

- the surface quality of a rolled part primarily depends on the reduction ratio  $\delta$  and the tool angle  $\theta$ ,
- the chuck velocity  $V_u$  and the forming angle  $\alpha$  have the smallest impact on the surface quality of a rolled part,
- the surface quality of a rolled part is reduced when the skew rolling process is conducted with low reduction ratios  $\delta$  and high tool angles  $\theta$ ,
- the use of the random forests model for predicting the waviness  $W_t$  makes it possible to obtain a high value of the coefficient of determination  $R^2$ ,
- the highest-fit model, i.e. the random forests model, makes it possible to reduce the time required for determining the initial parameters of the rolling process,

- further studies should be conducted to apply the obtained regression model results to skew rolling processes for stepped parts.

## Acknowledgments

The research was financed in the framework of the project: Development of new rolling technologies for rail axle forgings, No. LIDER/9/0060/L-12/20/NCBR/2021. Total cost of the Project: 1 466 831.25 PLN. The project is financed by the National Centre for Research and Development under the 12<sup>th</sup> edition of the LIDER Programme.

## REFERENCES

1. Meyer M., Stonis M., Behrens B.-A. Cross wedge rolling and Bi-directional forming of preforms for crankshafts. *Production Engineering Research and Development*. 2015; 9: 61–71.
2. Li Q., Lovell M. Cross Wedge rolling failure mechanisms and industrial application. *The International Journal of Advanced Manufacturing Technology*. 2008; 37: 265–278.
3. Yang H., Zhang L., Hu Z. The Analysis of the Stress and Strain in Skew Rolling. *Advanced Materials Research*. 2012; 538-541: 1650–1653.
4. Stefanik A., Morel A., Mróz S. Theoretical and Experimental Analysis of Aluminium Bars Rolling Process In Three-High Skew Rolling Mill. *Archives of Metallurgy and Materials*. 2015; 60: 809–813.
5. Cakircali M., Kilicaslan C., Guden M., et al. Cross wedge rolling of a Ti6Al4V (ELI) alloy: the experimental studies and the finite element simulation of the deformation and failure. *The International Journal of Advanced Manufacturing Technology*. 2013; 65: 1273–1287.
6. Pater Z., Tomczak J., Bulzak T., et al. Numerical and experimental study on forming preforms in a CNC skew rolling mill. *Archives of Civil and Mechanical Engineering*. 2022; 22(54): 1–21.
7. Pater Z., Tomczak J., Lis K., et al. Forming of rail car axles in a CNC skew rolling mill. *Archives of Civil and Mechanical Engineering*. 2020; 20: 1–13.
8. Wang J., Shu X., Zhang S., et al. Research on microstructure evolution of the three-roll skew rolling hollow axle. *The International Journal of Advanced Manufacturing Technology*. 2022; 118: 837–847.
9. Wang J.T., Shu X.D., Zhang S., et al. Research on variation law of workpiece temperature of three roll skew rolling hollow axle. *IOP Conf. Ser.: Materials Science and Engineering*. 2022; 1270: 1–6.

10. Shu X., Zhang S., Shu C., et al.: Research and prospect of flexible forming theory and technology of hollow shaft by threeroll skew rolling. *The International Journal of Advanced Manufacturing Technology*. 2022; 123: 689–707.
11. Pater Z., Tomczak J., Bulzak T. Problems of forming stepped axles and shafts in a 3-roller skew rolling mill. *Journal of Materials Research and Technology*. 2020; 9: 10434–10446.
12. Tomczak J., Pater Z., Bulzak T., et al. Design and technological capabilities of a CNC skew rolling mill. *Archives of Civil and Mechanical Engineering*. 2021; 21: 1–17.
13. Lechwar S., Rauch Ł., Pietrzyk M. Use of Artificial Intelligence in Classification of Mill Scale Defects. *Steel Research International*. 2015; 86(3): 266–277.
14. Kurra S., Rahman N.H., Regalla S.P., et al. Modeling and optimization of surface roughness in single point incremental forming proces. *Journal of Materials Research and Technology*. 2015; 4(3): 304–313.
15. scikit-learn. Available online: [https://scikit-learn.org/stable/supervised\\_learning.html#supervised-learning](https://scikit-learn.org/stable/supervised_learning.html#supervised-learning) (accessed on 19 June 2023)
16. dmlc XGBoost. Available online: <https://xgboost.readthedocs.io/en/stable/> (accessed on 19 June 2023)
17. SHAP. Available online: <https://shap.readthedocs.io/en/latest/> (accessed on 19 June 2023)